Climatic control on river discharge simulations, Mittivakkat Glacier catchment, Ammassalik Island, SE Greenland*

S.H. Mernild and B. Hasholt

Institute of Geography, University of Copenhagen, Øster Voldgade 10, DK-1350 Copenhagen, Denmark.
E-mail: *sm@geogr.ku.dk*

Received 30 January 2006; accepted in revised form 29 May 2006

Abstract A lumped conceptual Rainfall–Runoff Model (the NAM model) was applied to quantify simulated intra- and inter-annual discharge from the Mittivakkat glacier catchment (18.4 km^2, 78% glacier cover), Ammassalik Island, SE Greenland. Discharge simulations were performed for three periods: 1999–2004 (calibration period), 1993–1995 and 1998/1999 (validation period), and 2071–2100 (scenario period). In periods when observed winter discharges were lacking, visual observations from daily photographic time lapse were used for calibration. The timing and magnitude of simulated discharge were in general in good accordance with observed discharge ($R^2 = 0.77$). However, discrepancies between simulated and observed discharge occur (maximum daily difference up to 3.4 $m^3 s^{-1}$, up to 11% difference between observed and simulated cumulative discharge, and model predicted river break-up 1–3 d before it actually occurs). For the period 2071–2100 future IPCC A2 and IPCC B2 climate scenarios were used as input for NAM based on HIRHAM RCM and HadCM3 AOGCM model simulations. The IPCC scenarios indicated mean maximum monthly runoff higher than 900 mm w.eq., and mean annual runoff around 3200 mm w.eq. yr^{-1}, approximately one and a half times higher than the runoff in 1993–2004 of approximately 2000 mm w.eq. yr^{-1}. The increasing runoff indicated an approximately three times higher negative glacier net mass balance ranging from about -750 mm w.eq. yr^{-1} (1961–1990) to approximately -2000 mm w.eq. yr^{-1} (2071–2100).

Keywords Ammassalik; discharge; Greenland; HadCM3; HIRHAM; IPCC; lumped hydrological model; Mittivakkat Glacier catchment

Introduction

It is generally agreed that global warming is taking place (e.g. Kane 1997; Crowely 2000; WHO 2001; Box 2002; ACIA 2005; Sturm *et al.* 2005), which has caused increased melting of local glaciers in the Arctic, and an increased influx of fresh water to the oceans (e.g. ACIA 2005). Furthermore, simulations of future climate by Global Circulation Models (GCM) indicated an increase in global air temperature, and that warming will be more pronounced in northern latitudes (e.g. Maxwell 1997; Flato and Boer 2001; Rysgaard *et al.* 2003; ACIA 2005). Northeast Greenland Atmosphere–Ocean Models (AOM) indicated an air temperature increase of up to 4–8°C over the next 100 years (Rysgaard *et al.* 2003; ACIA 2005), with the largest changes in autumn and winter seasons (Sælthun and Barkved 2003). As a result, the contribution of fresh water from Eastern Greenland to the Greenland Sea and the Straits of Denmark will increase during this century. This flux of freshwater may affect the density-driven sinking of cold surface water, the thermohaline circulation, in the sea outside east Greenland (e.g. Broecker *et al.* 1985; Broecker and Denton 1990), combined

*Paper presented at the 15th Northern Research Basins Symposium/Workshop (Luleå and Kvikkjokk, Sweden), 29 August–2 September 2005.

doi: 10.2166/nh.2006.018

Nordic Hydrology **Vol 37 No 4–5 pp 327–346** © IWA Publishing 2006

with a pronounced reduction of sea ice within the Arctic sea, including the Greenland Sea (e.g. Serreze *et al.* 2002; Sturm *et al.* 2005). Furthermore, the influx of fresh water could be used for assessing the contribution of runoff to sea-level rise and for the addition of nutrients to the ocean (e.g. Tangborn 1984; Dowdeswell *et al.* 1997; Rysgaard *et al.* 2003; ACIA 2005). Changes in fresh water influx must be taken into account when planning hydroelectric power schemes and water supply (e.g. Hasholt 1980; Hock and Jansson 2005).

Discharge simulations based on the effect of climate control has been estimated and predicted earlier from glacierized and/or snow-covered areas (e.g. Gottlieb 1980; Bruland and Sand 1994; Bøggild *et al.* 1998, 1999; Bengtsson and Singh 2000; Bruland and Killingtveit 2002; Hock 2003; Hirashima *et al.* 2004). Computations of glacier discharge require an understanding of two main separate steps: (1) estimating the water input to the glacier, e.g. melt water production on snow covered and glacierized areas; and (2) routing of water (melt water and liquid (rain) precipitation) through snow/firn cover and glacier ice, transforming the input contributions into a runoff hydrograph at the glacier terminus based on seasonal changes in hydrological response. Melt water production is normally based on two methods: (a) energy balance calculations, which attempt to quantify melt as residual in the heat balance Equation (e.g. van de Wal and Russell 1994; Arnold *et al.* 1996; Hock and Hoetzli 1997; Hag *et al.* 2001; Bruland and Killingtveit 2002; Liston and Elder 2005; Garen and Marks 2005); and (b) temperature-index (degree-day) calculations, assuming an empirical relationship between air temperature (sensible heat) and melt rates (e.g. Bruland and Sand 1994; Braithwaite 1995; Bengtsson and Singh 2000; Hock 2003; Kuhn 2003; Hasholt and Mernild 2004). Despite their simplicity, the degree-day models have produced reasonable results for periods of several days and weeks. However, the accuracy decreases with increasing time resolution, e.g. hourly (e.g. Baker *et al.* 1982; Hock 1999). Attempts have been made to describe the drainage processes and the delay of runoff within the glacier. Water movement in and under a glacier are intrinsically complex and far less understood, because it involves the liquid phase (water) moving through the solid phase (ice) at the melting temperature, while the ice is deformable allowing englacier conduits to change size and shape (Hock and Jansson 2005). Campbell and Rasmussen (1973) described the whole glacier as a porous media, and later, for example, Hock and Hoetzli (1997), Jansson *et al.* (2003) and Hock (2003) described the glacier as a system of reservoirs, with different storage properties of the media: snow, firn, and ice. Despite their simplicity, the reservoir models tend to perform remarkably well (Jansson *et al.* 2003).

The goal of this study was to test the conceptual Rainfall–Runoff Model's (NAM) ability to simulate known intra- and inter-annual variability, in order to produce complete description of runoff in time from a snow and glacierized catchment, SE Greenland, where incomplete recordings occur due to harsh climatic conditions and logistics difficulties and, furthermore, to predict future changes in runoff regime and in storage. We performed the model simulations with the following specific objectives: (1) to discuss the simple, and the non-model, incorporated snow related routines and glacier runoff response routines significant for the high-arctic hydrological cycle; (2) to simulate intra- and inter-annual variability in runoff for the calibration period (1999–2004) and validation period (1993–1995 and 1998/1999); (3) to validate and calibrate simulated winter runoff with visual photographic time lapse observations where observed discharges were lacking; and (4) finally to use HIRHAM regional climate model (RCM) output parameters based on the future IPCC A2 and B2 scenarios as input parameters in the NAM model to simulate average monthly runoff and change in storage for the scenario period (2071–2100).

Study area

Physical settings

The Mittivakkat Glacier complex (31 km^2) (65°42′N latitude; 37°48′W longitude) is located on Ammassalik Island, Southeast Greenland, approximately 15 km northwest of the town Tasiilaq (Ammassalik) and 50 km east of the eastern margin of the Greenland Ice Sheet, separated from the mainland by the 10–15 km wide Sermilik Fiord. The Mittivakkat Glacier catchment (18.4 km^2) is drained by the glacier outlet from the southwestern part of the Mittivakkat Glacier through a proglacial valley (Figure 1). The catchment is characterized by a strong alpine relief, and ranges in elevation from 0 to 973 m a.s.l., with highest altitudes in the eastern part of the catchment. Avalanches near the glacier are rare. The catchment is covered by parts of the Mittivakkat Glacier complex (78%; 14.4 km^2), a temperate glacier ranging from approximately 160–930 m a.s.l. in elevation. Since the first observation in 1933, the glacier terminus has retreated about 1.2 km, with a decrease in glacier surface elevation up to 100 m (below the 300 m a.s.l. elevation) (e.g. Valeur 1959; Fristrup 1961; Hasholt 1986, 1988, 1992; Knudsen and Hasholt 2004). The average winter mass balance, summer mass balance, and net mass balance (1995–2003) are, respectively, 1.27 m w.eq., −1.80 m w.eq., and −0.53 m w.eq., showing a negative net mass balance (Knudsen and Hasholt 2004; Mernild *et al.* 2006b). Approximately 22% of the catchment is covered by bedrock (in higher elevations), loose sediments as talus and debris flow deposits (in lower elevations) and moranic deposits or sediment of fluvial origin in the proglacial valley bottoms.

Climate

The Mittivakkat Glacier area climate is an ET, tundra climate, according to the Köppen classification system. Two main meteorological stations are located within the catchment: Station Nunatak (515 m a.s.l.) and Station Coast (25 m a.s.l.) (Figure 1). Based on data from these stations, mean annual air temperature (MAAT) for the area is −1.6°C (1999–2004), maximum monthly average is 4.9°C in July and minimum is −7.6°C in February. The mean annual relative humidity is 88% (1999–2004). The total annual precipitation sum (liquid and solid) at Station Nunatak is 1767 mm w.eq. yr^{-1} and 1312 mm w.eq. yr^{-1} at Station Coast (1999–2004). Between 65–85% of the TAP falls as snow from approximately mid-September to late May. The mean annual wind speed is 4.0 m s^{-1} (1999–2004), mainly dominated by N and E winds during autumn, winter, and spring, and SW, S, and E winds during summer. Wind velocity during katabatic winds (*piteraq*) can gust up to 85 m s^{-1} (Mernild *et al.* 2006b).

Hydrological response

In the end of the winter season and beginning of melt season, melting from a snow pack on,for example, bedrock/rock and glacier ice often does not cause runoff (i.e. no hydrological response), due to internal refreezing of percolating surface melt water (e.g. Marsh and Woo 1984; Trabant and Mayo 1985; Conway and Benedict 1994; Marsh 1999; Bøggild 2000; Bøggild *et al.* 2005). Latent heat from internal refreezing of water heats up snow and firn layers to a maximum 0°C (isothermal) through the melt season (e.g. Trabant and Mayo 1985; Conway and Bennedict 1994), resulting in an increasing proportion of runoff (i.e. hydrological response). After melting the snow cover through summer season, exposed glacier ice and bedrock results in a relatively rapid hydrological response, giving high surface peak flow after daily glacier surface melt and liquid (rain) precipitation events. On the glacier surface inter-rill flow is initially dominated by the surface gradient, and further downwards by the gradient, orientation, and size/form of fissures and surface channels. After entering into the glacier, the englacial flow is dominated by the potential gradient, orientation, size/form of crevasses (e.g. Fountain *et al.* 2005), and the orientation and evolution of englacial and subglacial drainage systems through the melt season

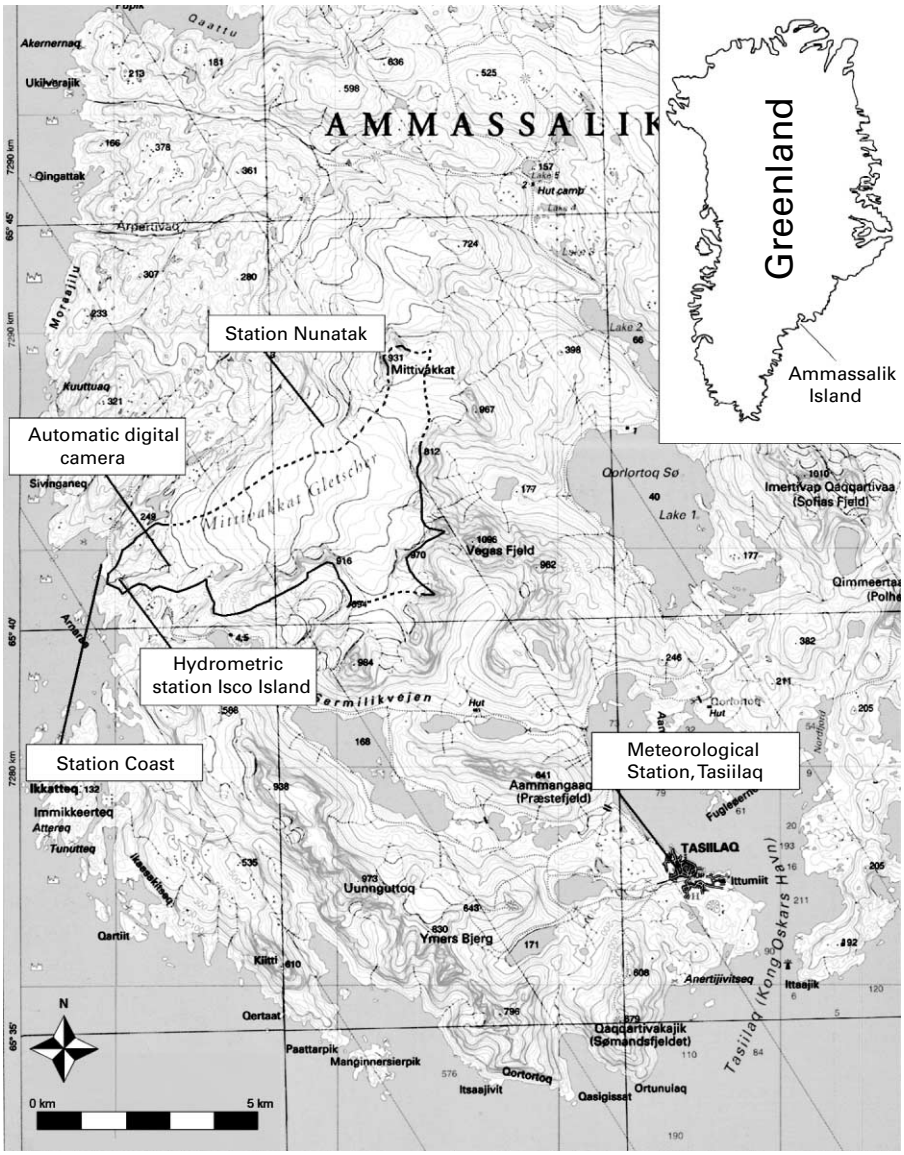

Figure 1 Location map showing the Mittivakket Glacier catchment (18.4 km^2), Ammassalik Island, including the hydrometric station at Isco Island located in the pro-glacial valley. The automatic digital camera takes daily photos (at 12 noon) of the pro-glacial valley, the meteorological stations at Station Nunatak and Station Coast and the Meteorological Station in Tasiilaq (Ammassalik). The dashed line indicates the non-stable topographic watershed divide on the Mittivakkat Glacier, and the full line the topographic watershed divide on bedrock for the Mittivakkat Glacier catchment. The inset figure indicates the general location of the Mittivakkat Glacier catchment within Eastern Greenland. (Modified after Greenland Tourism)

(e.g. Shreve 1972; Röthlisberger 1972; Röthlisberger and Lang 1987; Hock and Hooke 1993; Fountain and Walder 1998). On bedrock the impermeable conditions result in rapid hydrological response, giving high surface peak flow and no base flow discharge. The loose sediments, debris flow deposits, and morainic/fluvial deposits result in relatively lower responding hydrological response, giving lower amounts of overland flow and contributions from subsurface flow.

Methods

The NAM Rainfall–Runoff Model is a conceptual lumped model (Nielsen and Hansen 1973; DHI 2003a, b) describing in a simple quantitative form the behavior of the land phase hydrological cycle by a set of linked mathematical statements by simulating hydrological processes as: overland-flow, inter-flow, and base-flow components as a function of the moisture content in four different interrelated reservoirs representing: snow storage (seasonal and perpetual snow storage), surface storage (moisture intercepted on vegetation and water trapped in surface depressions), root zone storage (soil moisture in root zone), and groundwater storage (Figure 2). The NAM model was originally developed for Danish catchments, not for glacierized catchments. The occurrence of a glacier is incorporated in the NAM simulations as a snow storage given analog physical dimensions (e.g. thickness and location m a.s.l.) and hydrological characteristics (e.g. irreducible liquid (water) content). Furthermore, a number of snow processes and glacier runoff response processes are not incorporated in the NAM model, e.g. sublimation (phase change processes, vertical flux), water retention in snow/firn and on glacier ice generating ice lenses and superimposed ice respectively, seasonal minimizing of snow cold content, seasonal changes in internal glacier drainage system, and processes related to release of englacial bulk water storage.

NAM runoff simulations for the Mittivakkat Glacier catchment require basic input information: catchment dimensions (area and hypsometric characteristic), hydrological catchment characteristics (runoff parameters, storage content, storage thresholds, and routing constants), climatic conditions (lapse rates and time series of varying meteorological data obtained from stations within or adjacent to the study area), and initial conditions (e.g. snow distribution and the hydrological catchment variables).

Snow routine in NAM

Snow accumulation and melt significantly affect hydrological processes in Arctic catchments where the snow pack acts as a storage in which precipitation is retained during the cold season and subsequently released as melt water during warmer parts of the year. A description of the snow routine in NAM (DHI 2003a) shows that precipitation enters directly into the surface storage as liquid (rain) precipitation during periods with air temperatures above a certain base level (T_0). During periods with air temperature below T_0, precipitation (solid (snow) precipitation) is retained in the snow storage (Figure 2) from which it melts in periods with air temperatures above T_0. The shift between liquid (rain) precipitation and solid (snow) precipitation takes place at T_0.

Wind pattern around topography characteristics (ridge and peaks) allow significant wind re-distribution of snow due to high wind speeds. Snow re-distribution processes are partly incorporated in NAM, not in relation to topography but to elevation characteristics. To avoid unrealistic accumulation of snow a user-specified upper limit of snow storage in each individual elevation zone is used. Snow storage exceeding this value will be transferred to the neighbouring lower zone (DHI 2003b).

The snowmelt is calculated using a degree-day approach. The generated melt water is retained in the snow storage as liquid water until the total amount of water exceeds the irreducible liquid content. When the air temperature is below T_0: (1) the liquid water content in the snow storage freezes; and (2) evaporation from the snow pack is neglected (DHI 2003a).

Model setup and application

For the Mittivakkat NAM model all four reservoirs were used (Figure 2). The following snow and catchment characteristics were specified (Table 1): (1) subdivision of the catchment into ten altitude distributed snow storages for each 100 m elevation; (2) from

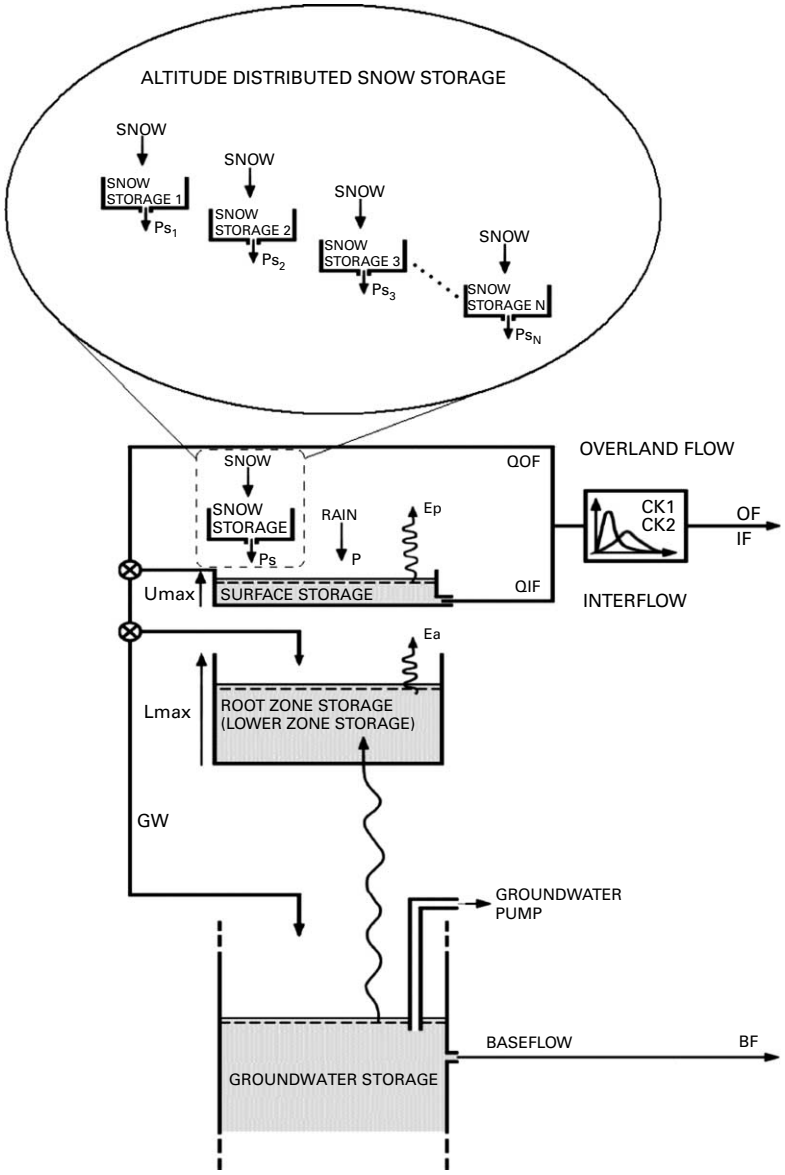

Figure 2 Simple structure of the NAM model with extended altitude distributed snow routine. (Modified after DHI 2003a)

observations a minimum snow depth on 0.5 m for full snow coverage was used on bedrock/rock (below 200 m a.s.l.) (Mernild *et al.* 2006b). When the snow depth is below 0.5 m the area coverage and snow melt will be reduced linearly; (3) from snow observations irreducible liquid content on 7–8% of pore space was found (Mernild *et al.* 2006a), comparable with estimates (3–7% of pore space) by Colbeck (1974) and Bøggild (1989). Here, irreducible liquid content of total volume is needed, observed values were re-calculated and irreducible liquid content values on 5% of total volume was used; (4) from meteorological observations at Station Nunatak and Station Coast (1999–2004) a mean annual air temperature lapse rate of -0.24°C 100 m^{-1} was applied (Mernild *et al.* 2006b), covering a yearly variation from -0.51 (February) to 0.33°C 100 m^{-1} (July) controlled by a change in wind regime throughout the year due to summer sea breezes in the coastal area

Table 1 User-defined set-up constants in the snow model routine (for parameter definitions see DHI (2003a, b))

Symbol	Value	User defined set-up constants in the snow model routine
–	10	Altitude-distributed catchment zones for each 100 m a.s.l.
		Monthly degree-day coefficient (mm w.eq. $C^{-1}\,d^{-1}$):
C_{snow}	2.0	Winter (September through May)
	3.7	Summer (June through August).
T_0	0	Base air temperature level (°C)
–	−0.24	Mean annual air temperature lapse rate (°C 100 m^{-1}) (Mernild *et al.* 2006b).
–	93	Mean annual precipitation lapse rates for solid and liquid precipitation (mm w.Equation 100 m^{-1}).
–		Minimum snow storage depth for full coverage (mm w.eq.) (Hasholt and Mernild 2004; Mernild *et al.* 2006b)
	500	< 200 m a.s.l. (bedrock, non-glaciericed area)
–		Maximum snow storage depth in zones (mm w.eq.) (Mernild *et al.* 2006b)
	2000	< 700 m a.s.l.
	1500	700 m a.s.l. to 800 m a.s.l.
	1400	> 800 m a.s.l.
–	5	Maximum irreducible liquid content (% of total volume) (Mernild *et al.* 2006a)
–		Initial snow cover (glacier) location and thickness for calibration and validation periods
	200	Elevation zones above (m a.s.l.)
	115	Glacier thickness (m)
–		Initial snow cover (glacier) location and thickness for scenario period
	300	Elevation zones above (m a.s.l.)
	75	Glacier thickness (m)

(Mernild *et al.* 2005, 2006b); (5) the base level (T_0) was set to be 0°C; (6) monthly degree-day factor of 2.0 mm w.eq. $°C^{-1}\,d^{-1}$ (for the snow covered period September through May) and 3.7 mm w.eq. $°C^{-1}\,d^{-1}$ (for the glacier ice covered period June through August) were used due to changes in surface characteristics (albedo), which were approximately half the values of degree-day factors for snow and ice found on West Greenland by Braithwaite (1995); and (7) initial mean snow cover thickness of 115 m for elevation zones above 200 m a.s.l., based on the average glacier thickness measured by radio-echo sounding observations by Knudsen and Hasholt (1999). For the scenario period (2071–2100), an initial snow cover thickness of 75 m for elevation zones above 300 m a.s.l. was used representing the glacier. The scenario snow thickness was based on melt caused by air temperature changes from 2004–2071, based on linear regression between changes in air temperature and glacier terminus/mass from 1933 through 2004. For parameter definitions see DHI (2003a, b).

Climate, climate-related and discharge input data

The driving variables in the NAM model are time series of: precipitation, air temperature, and potential evapotranspiration for the periods: 1999–2004 (calibration period), 1993–1995 and 1998/1999 (validation period), and 2071–2100 (scenario period). For model calibration and validation observed daily discharge was obtained. Yearly simulation period goes from September through August the following year, due to the annual cycle of the Mittivakkat glacier net mass balance (Knudsen and Hasholt 2004; Mernild *et al.* 2006b). The simulations were performed with daily time steps.

Input data for 1999–2004 and 1993–1999. Precipitation input consists of liquid and solid precipitation. Liquid (rain) precipitation was measured at Station Nunatak approximately 0.45 m

above ground and solid (snow) precipitation was calculated from the ultrasonic snow-depth sounder observations (Campbell SR50) at Station Nunatak. To estimate the snow water equivalent (SWE) precipitation noise was removed from the sounder data. The remaining snow-depth increases were adjusted by a temperature-dependent snowflake density (Brown *et al.* 2003) and an hourly snow pack settling rate (Anderson 1976). Snow settles as it accumulates and thus the depth of snow on the ground is always less than the initial amount of snowfall. Station Nunatak SWE precipitation was calibrated against observed Mittivakkat Glacier winter mass balance, to account for the wind effect, due to the station's exposed location at the highest peak on the small nunatak (< 5 m from the glacier margin in the dominating wind direction) (Mernild *et al.* 2006b).

Air temperature (2 m) was measured at Station Nunatak. Mean annual air temperature lapse rates were calculated based on air temperature data (2 m) from Station Nunatak and Station Coast (1999–2004) (Figure 1 and Table 1) (Mernild *et al.* 2006b).

Potential evapotranspiration was calculated based on the Makkink formula (1957), using incoming short-wave radiation (4 m) and air temperature from Station Nunatak. The Makkink formula was chosen because it previously has been used in, for example, Denmark, The Netherlands, and in the Czech Republic with reasonable results (e.g. Aslyng and Hansen 1982; Jacobs and de Bruin 1998; de Bruin and Lablans 1998; Dubrovský *et al.* 2002; Plauborg *et al.* 2002).

Discharge was calculated from stage-discharge relationships estimated each year (R^2 values from 0.91 to 0.99), formed from a regression analysis using observations at the Isco Island hydrometric station (Figure 1). The discharge cross section has been stable for approximately 30 years, yielding an assumed 10–15% accuracy when a single discharge measurement is used (Hasholt and Mernild 2004; Mernild 2006).

Input data for 2071–2100 (The HIRHAM Regional Climate Model). The IPCC A2 and B2 climate scenarios (www.ipcc.ch) were used in the HIRHAM RCM (Christensen *et al.* 1996, 2001) for 2071–2100 (HIRHAM scenario period). The HadCM3 AOGCM (atmosphere–ocean general circulation model) (Gordon *et al.* 2000; Pope *et al.* 2000) was used as boundary conditions for the HIRHAM.

The HIRHAM output data were generated in 360 days (12 × 30 d) as mean daily values for a 50 km grid cell increment covering the Ammassalik Island. In normal years, five days were added, while six days were added for leap years. The extra days were added in between the existing 15th and 16th day in the following months: February (only in leap years), May, July, August, October, and December. Data values on the new days were calculated as an average of the previous and the following days. Before the HIRHAM RCM output data can be trusted for any practical use, it needs to be tested against observed climate data (HIRHAM control period, 1961–1990). The overall working assumption is that, if the model can reproduce the past (1961–1990), then it can be trusted to estimate the future (2071–2100). Climate data from Station Nunatak extends back to 1993; therefore, a regression function between Station Nunatak and the DMI station data from the town Tasiilaq were applied (1993–2004) (for DMI station location see Figure 1) to calculate data back to 1961.

Monthly HIRHAM modeled air temperature and precipitation (1961–1990) were tested against observed air temperature and precipitation at Station Nunatak (showing not significantly identical values ($p < 0.05$)), and furthermore calibrated against the observed data (the offset) from Station Nunatak. Mean monthly offset (calibration factors) between modeled and observed air temperature are shown in Figure 3 as an example, illustrating monthly variation ranging from −6.2°C (March) to 1.0°C (July), averaging −2.9°C. After calibration HIRHAM mean annual air temperature (MAAT) was −1.6°C (1961–1990), significantly identical ($p < 0.01$) with observed Station Nunatak MAAT (1961–1990). For the IPCC A2 and B2 scenarios (2071–2100) calibrated MAAT were −0.3°C and −0.2°C, respectively. HIRHAM RCM calibrated mean annual precipitation sum was 1669 mm w.eq. yr^{-1} (1961–1990), while the

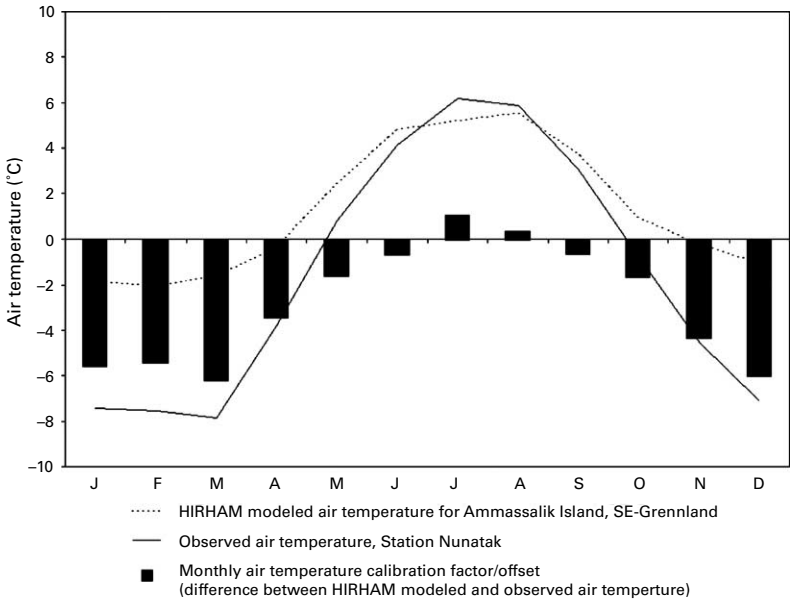

Figure 3 An example of monthly air temperature modeled by the HIRHAM RCM model, observed at Station Nunatak, and the monthly air temperature calibration factor (offset) based on the period 1961–1990

IPCC A2 and B2 scenarios (2071–2100) indicate a mean annual precipitation sum of 1635 mm w.eq. yr^{-1} and 1712 mm w.eq. yr^{-1}, respectively.

Makkink estimated potential evapotranspiration using HIRHAM modeled incoming short-wave radiation and air temperature was tested against Station Nunatak calculated potential evapotranspiration; showing not significantly identical values ($p < 0.05$). Therefore, modeled potential evapotranspiration was calibrated against observed values (the offset) based on monthly calibration factors. Calibrated mean annual potential evapotranspiration was 381 mm w.eq. yr^{-1} (1961–1990), while the IPCC A2 and B2 scenarios (2071–2100) indicate a mean annual potential evapotranspiration sum of 431 mm w.eq. $yr^{-1}$and 445 mm w.eq. yr^{-1}, respectively. An examination of the evapotranspiration as a function of latitude (from watersheds at latitudes from 44°N to 80°N) shows that the evapotranspiration is relatively high for the Mittivakkat catchment (Kane and Yang 2004). However, the Makkink formula was used, for example, in Denmark with reasonable results.

NAM model calibration and validation

A split-sample test was applied for calibration and validation of the modeled discharge (e.g. Klemes 1985, 1986; Refsgaard and Knudsen 1996; Refsgaard 2000; Refsgaard and Henriksen 2004). The calibration (1999–2004) was performed by auto-calibration so simulated discharge including high flows (peak flows) corresponds to observed discharges. Visual inspection of simulated and observed hydrographs, balance test of cumulative discharge volumes between simulated and observed hydrographs, and R^2 values were used for calibration and validation. The NAM model was validated against 1993–1995 and 1998/1999 only, because observed discharge was not available from 1995/1996 through 1997/1998.

Results

Calibration and validation periods

Table 2 presents observed and simulated runoff for the calibration period. A full year comparison between observed and simulated runoff is impossible due to missing discharge

Table 2 Observed discharge and simulated discharge from the Mittivakkat Glacier catchment, together with maximum daily difference in observed and simulated discharge (1999–2004). (*)The period is equal for daily simulated discharge and observed discharge

	Period with observed discharge	Sum observed runoff (mm w.eq.)	Sum simulated runoff (mm w.eq.)(*)	Difference between sum observed and sum simulated runoff (%)	Max daily difference in observed and simulated discharge ($m^3 s^{-1}$)
2000	8 Jun–17 Sept	2010	2062	2.1	2.6
2001	18 Jun–15 Sept	1726	1922	11.4	2.3
2002	10 Jun–5 Sept	1871	1742	−6.9	3.4
2003	7 Jun–20 Aug	927	938	1.2	1.9
2004	14 Jun–27 Aug	1907	1968	3.2	3.2

measurements in the beginning/end of the runoff season due to logistic difficulties. The observed runoff period varies from year to year. A comparison between observed and simulated runoff showed an annual average overestimation varying from 11.4% (2001) to −6.9% (2002), and a R^2 value of 0.79, $p < 0.01$ (p is the level of significance). A comparison of daily observed and simulated discharge values illustrates a maximum difference from 1.9 $m^3 s^{-1}$ (67%) (2003) to 3.4 $m^3 s^{-1}$ (44%) (2002) (Table 2 and Figure 4).

Annual variations (September through August) in simulated discharge are shown in Figure 4 (1999–2004). Timing and magnitude of simulated discharge are generally in good accordance with observed discharge, except for simulated peak discharges in June and July 2002 and 2004 which are underestimated by approximately 2–3 $m^3 s^{-1}$ (Table 2). From October/November through April/May (through winter) simulated runoff events occur in relation to hot spell melt events (Føhn winds) and liquid (rain) precipitation events.

No observed runoff values through winter periods occurred (1999–2004). Therefore, all simulated winter runoff events (during and/or after hot spells and liquid precipitation events) were validated using daily photographic time lapse taken at 12 noon of the pro-glacial valley. In Figure 4 examples of simulated winter runoff events are shown by the letters A to G, and in Figure 5 photos were used to check the occurrence of runoff in the valley. The photos A, B, D, E, F and G confirmed the occurrence of simulated runoff in the valley through winter, while photo C did not confirm the occurrence of simulated runoff. Furthermore, snow surface

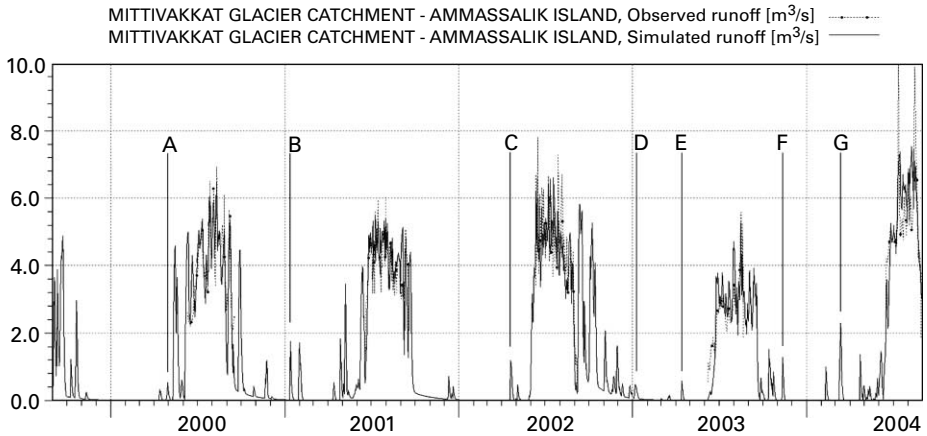

Figure 4 Observed and simulated discharge from the Mittivakkat Glacier catchment, Ammassalik Island, from August 1999 through September 2004. The letters A to G refer to daily photographic time lapse from Fig. 5, confirming and not confirming the occurrence of runoff during and after hot spells, events and liquid precipitation events through winter

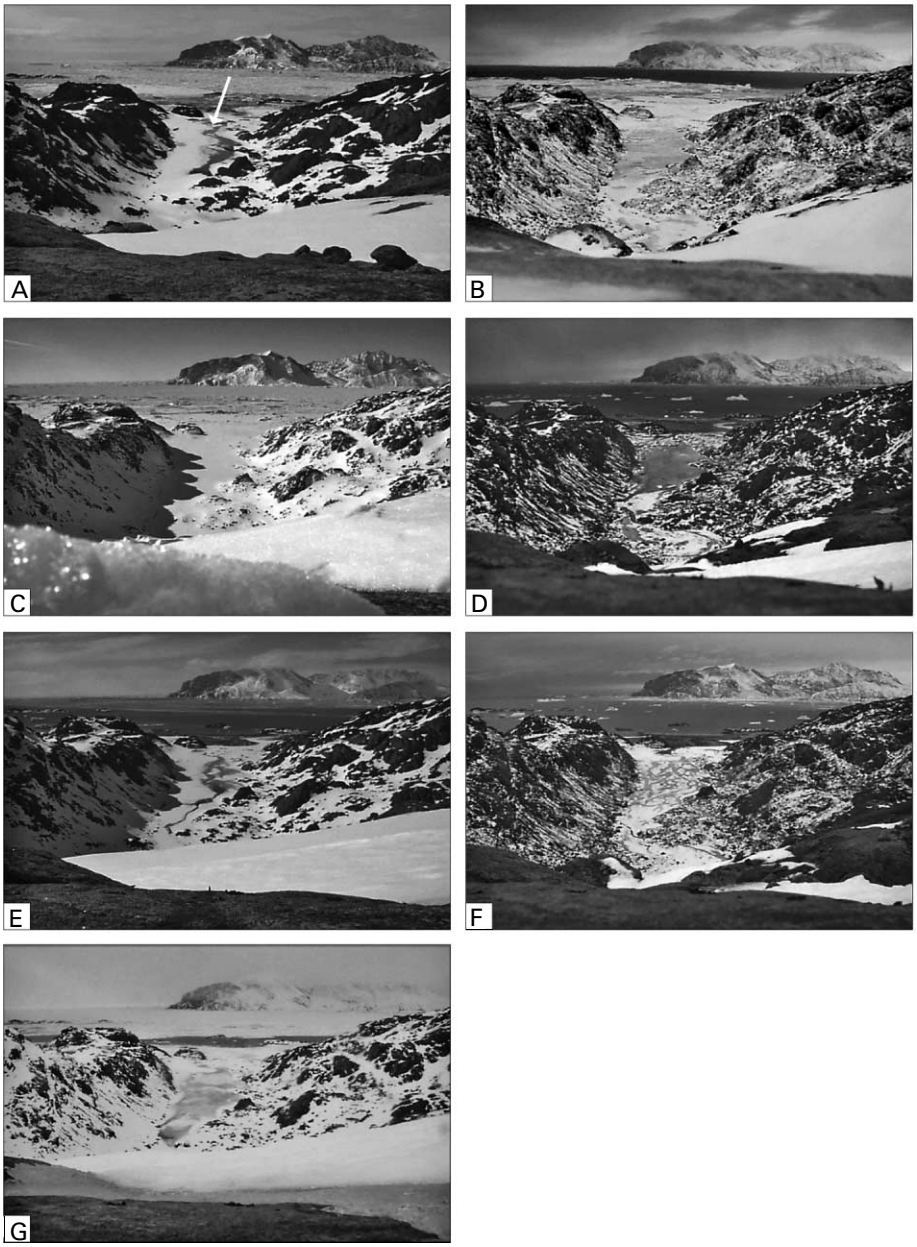

Figure 5 Photographic time lapse of the pro-glacial valley at 12 noon, including the location of the Isco Island hydrometric station (see arrow on photo A). Photos A, B, D, E, F and G confirm the occurrence of runoff from the Mittivakkat Glacier catchment on April 29, 2000; January 31, 2001; January 4, 2003; April 19, 2003; November 10, 2003; and March 12, 2004 respectively. Photo C does not confirm the occurrence of runoff on April 25, 2002

depressions were not seen in the valley on photo C, therefore there was no reason to believe that runoff had taken place under the snow cover, e.g. as tunnel flow. Explanations for simulated runoff not being confirmed by photo were probably that surface melt water: (1) percolated into the snow/firn pack, got stored as refrozen water as ice lenses and/or at the glacier surface as superimposed ice due to the cold content (Bøggild *et al.* 2005); and/or (2) went into englacial reservoirs (pockets). Table 3 shows the calculated amount of simulated runoff not confirmed by daily photos through the period 1999–2004, which varies

Table 3 Simulated and observed date for river break-up, amount of trapped runoff in winter, and annual sum of simulated runoff from the Mittivakkat Glacier catchment (1999–2004)

	Simulated date for river break-up (continuous discharge)	Date for river break based on photos from the pro-glacier valley	Simulated sum of runoff possible trapped in the snow pack or at the ice surface through winter (mm w.eq. yr^{-1}). The percent (%) is in relation to the annual sum of simulated discharge	Annual sum simulated runoff from Mittivakkat Glacier Catchment (mm w.eq. yr^{-1})
1999/2000	11 May	13 May	28 (1.2%)	2145
2000/2001	23 May	26 May	224 (10.0%)	2282
2001/2002	27 May	28 May	80 (4.4%)	1987
2002/2003	8 Jun	10 Jun	16 (1.2%)	1326
2003/2004	25 May	26 May	32 (1.6%)	2190
Average	–	–	76 (3.6%)	1986

from 16 mm w.eq. yr^{-1} in 2002/2003 to 226 mm w.eq. yr^{-1} in 2000/2001, averaging 76 mm w.eq. yr^{-1} (3.6%) (1999–2004). Calculated annual simulated runoff from the Mittivakkat Glacier catchment varies from 1326 mm w.eq. yr^{-1} (2002/2003) to 2282 mm w.eq. yr^{-1} (2000/2001), averaging 1986 mm w.eq. yr^{-1} (1999–2004) (Table 3). Furthermore, simulated date for river break-up (defined as days with subsequent continuous discharge) is compared with daily photos, indicating simulated date for river break-up 1–3 d before observed river break-up (Table 3).

Table 4 and Figures 6(a–d) present observed and simulated runoff for the validation period (1993–1995 and 1998/1999), a comparison showing an annual average over-estimation varying from 10.5% (1994) to −8.2% (1993), and a R^2 value of 0.77, $p < 0.01$. The maximum difference between daily observed and simulated discharge varies from 2.0 $m^3 s^{-1}$ (50%) (1994) to 3.4 $m^3 s^{-1}$ (39%) (1995).

Annual simulated runoff from 1993 through 1999 (September through August) is shown in Table 5. No photographic time lapse exists for this period for confirmation of simulated winter runoff. Therefore, the average value of 76 mm w.eq. yr^{-1} was used for water stored within the glacier, because the cold content is directly controlled by winter climate (air

Table 4 Observed and simulated runoff from the Mittivakkat Glacier catchment, together with maximum daily difference in observed and simulated discharge (1993, 1994, 1995, and 1999). (*)The period is equal for daily simulated discharge and observed discharge

	Period with observed discharge	Sum observed runoff (mm w.eq.)	Sum simulated runoff (mm w.eq.)(*)	Difference between sum observed and sum simulated runoff (%)	Max daily difference in observed and simulated discharge ($m^3 s^{-1}$)
1993	1 Sept–21 Sept	382	350	−8.4	2.8
1994	30 Jun–28 Aug	1307	1444	10.5	2.0
1995	1 Jul–31 Aug	1896	1811	−4.5	3.4
1996	No data	No data	No data	No data	No data
1997	No data	No data	No data	No data	No data
1998	No data	No data	No data	No data	No data
1999	22 Jun–31 Aug	937	1018	8.6	3.2

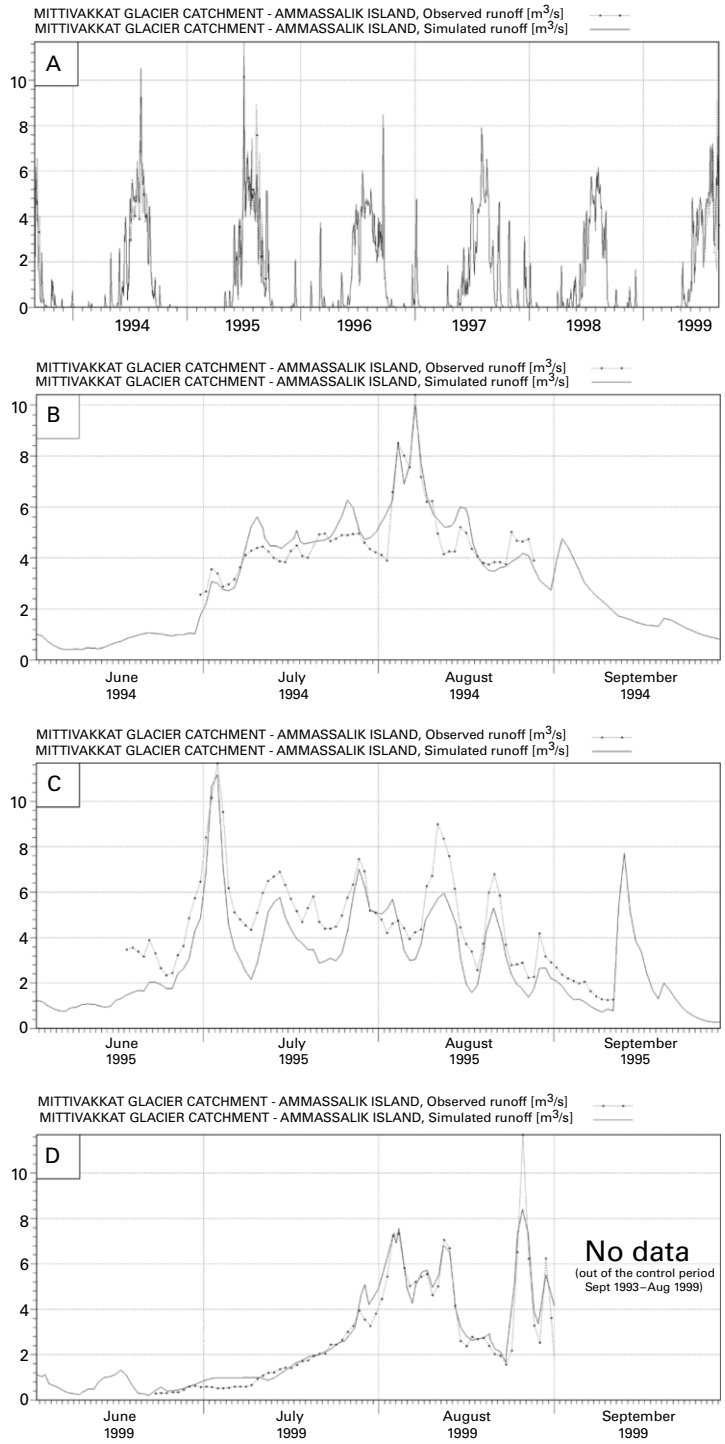

Figure 6 (a) Observed and simulated discharge from the Mittivakkat Glacier catchment, Ammassalik Island, from August 1993 through September 1999. However, observed discharge was missing for 1996, 1997, and 1998; and (b–d) are close-up pictures of the observed and simulated discharge from June through September for 1994, 1995, and 1999, respectively

Table 5 Simulated date for river break-up and annual sum of simulated runoff from the Mittivakkat Glacier catchment

	1993–1994	1994–1995	1995–1996	1996–1997	1997–1998	1998–1999	Average
Simulated date for river break-up (continuous discharge)	22 May	27 May	28 May	17 May	10 May	23 May	–
Annual sum simulated runoff from Mittivakkat Glacier Catchment (mm w.eq. yr^{-1})	2144	2091	1864	2126	1914	1639	1963

temperature) penetrating into the snow/firn pack (Bøggild *et al.* 2005), and statistically mean air temperature from 1999–2004 and 1993–1999 was significantly identical ($p < 0.05$).

Annual simulated runoff is estimated from 1639 mm w.eq. yr^{-1} (1998/1999) to 2144 mm w.eq. yr^{-1} (1993/1994), averaging 1963 mm w.eq. yr^{-1} (1993–1999) (Table 5), which is significantly identical ($p < 0.05$) with simulated runoff from 1999–2004 (1986 mm w.eq. yr^{-1}), indicating an increase in runoff of around 1%. Simulated date for river break-up (1993–1999) varies approximately within three weeks from 10 May (1997/1998) through 28 May (1995/1996) (Table 5).

Scenario period

Table 6 indicates an increase in mean annual runoff of 56% from 2039 mm w.eq. yr^{-1} (1961–1990) to 3181 mm w.eq. yr^{-1} (2071–2100) for the IPCC scenario A2, and of 58% from 2039 mm w.eq. yr^{-1} to 3234 mm w.eq. yr^{-1} for the IPCC scenario B2. The monthly maximum runoff for the IPCC A2 and B2 scenarios occurs in July and August with values around 900 mm w.eq., values approximately 300 mm w.eq. higher for corresponding months (1961–1990). The increasing runoff indicates an increasing negative glacier net mass balance from -751 mm w.eq. yr^{-1} (1961–1990) to -1977 mm w.eq. yr^{-1} for the IPCC A2 and -1967 mm w.eq. yr^{-1} for the IPCC B2.

Table 6 Mean monthly and annual simulated runoff from the Mittivakkat Glacier catchment, based on the HIRHAM RCM output data from 1961–1990 and from the IPCC A2 and B2 climate scenario (2071–2100)

	Runoff HIRHAM control period after calibration, 1961–1990 (mm w.eq.)	Runoff IPCC scenario A2, 2071–2100 (mm w.eq.)	Runoff IPCC scenario B2, 2071–2100 (mm w.eq.)
September	270	461	445
October	58	122	116
November	15	53	56
December	5	12	12
January	4	4	4
February	5	5	5
March	3	4	6
April	20	54	54
May	81	152	159
June	355	492	510
July	594	887	950
August	629	936	917
Sum	2039	3181	3234

Discussion

The NAM Rainfall–Runoff Model was chosen because of its simplicity and robustness. It demands rather few input data which is important for the applicability both for calculating discharge for earlier periods and for future scenarios produced by regional climate models which do not always produce a full description of the meteorological situation. It appears that our choice of a simple methodology provides estimates of the runoff which are in good accordance with observed runoff although a number of snow and glacier runoff response processes significant for the high-latitude hydrological cycle are not incorporated in the model. The authors are aware of the model limitations, and below are given examples from more detailed studies illustrating and quantifying, if possible, where processes not accounted for in the model will affect the results.

Blowing-snow and sublimation model simulations for the Mittivakkat Glacier catchment by Hasholt *et al*. (2003) and Mernild *et al*. (2006b) show significant snow redistribution and sublimation losses of 12–15% of annual precipitation ($\sim$150–200 mm w.eq. yr^{-1}) to the atmosphere. The snow routine in NAM incorporates accumulation and re-distribution of wind-transported snow to the lower neighbouring elevation zone, only influenced by elevation, and not in response to both elevation and topographic influences, which according to previously mentioned studies significantly influence the snow processes in the catchment. Together with the not included sublimation routines this may affect uncertainties in the high-latitude hydrological cycle including the runoff hydrograph in quantity, timing, and variability.

The NAM model use mean annual air temperature lapse rate to account for the altitudinal spatial variations in air temperature. A mean annual lapse rate of -0.24°C 100 m^{-1} was used: however, the monthly values vary between -0.51°C 100 m^{-1} for February and 0.33°C 100 m^{-1} for July (1999–2004) (Mernild *et al.* 2005, 2006b). These positive monthly values are governed by daytime summer sea breezes in the coastal area. The use of a fixed air temperature lapse rate in NAM ignores the daily lapse rates variation based on the frequent occurrence of a persistent temperature inversion in the area (approximately 300 m a.s.l., observed by radiosonde data). A fixed lapse rate value (-0.24°C 100 m^{-1}) appears useful in this study because it seems unlikely that air temperature would increase with elevation over the glacier surface atmospheric layer itself.

The NAM model operates with a certain melt threshold ($T_0 = 0$°C) and a fixed monthly degree-day factor for the entire catchment through winter and summer on 2.0 and 3.7 mm w.eq. °C^{-1} d^{-1}, respectively. Through the ablation period, the snow line moves up-glacier, changing the spatial distribution of surface characteristics to more exposed ice and less snow cover. Using the same monthly degree-day factor for the entire glacier causes spatial uncertainties in melt rates and furthermore in the high-latitude hydrological cycle through the ablation period, due to changes in surface characteristics (albedo) from snow to exposed ice cover.

Minimizing the snow cold content through the ablation period, trapping of percolating water by capillary forces, subsequent refreezing of trapped water in the snow/firn pack (as ice lenses) or at the ice surface (as superimposed ice) and the occurrence of snow damming are routines/issues not integrated into NAM. Therefore, simulated hydrological response is faster than observed, most pronounced in the beginning/end of the accumulation period. Simulated yearly break-up occur 1–3 d before observed break-up. Throughout the ablation period the difference between simulated and observed response will be minimized going towards isothermal snow conditions (0°C) and a snow-free stream bed.

Temporal storage/release of englacial bulk water, changes in the glacier topographic watershed divide (Figure 1) and in the internal drainage system due to glacier dynamics (internal deformation and basal sliding) are issues not incorporated into NAM, which affect

uncertainties in the hydrological cycle. Dye tracer experiments described in Mernild (2006) confirm englacial and subglacial water flow through crevasses, moulins, and tunnels (the internal drainage system) to neighboring glacier catchments, and modeling studies (Hasholt unpublished data) indicate that the northern catchment boundary located on the Mittivakkat Glacier itself is not well defined; therefore, the glacier may receive and deliver water across this boundary.

Runoff modeling on glacierized basins differs from conventional hydrological modeling, because glaciers significantly modify the runoff hydrograph in quantity, timing, and variability: (1) by temporarily storing water as snow, firn, and ice on different time scales; and (2) by changing the diurnal surface melt water cyclicity, routing the water through a decreasing seasonal snow cover as the area of exposed ice increases, and through the ice as the efficiency of the internal drainage system evolves during the melt season. In NAM routing of water through the glacier (through the snow cover, firn cover, and the ice) is performed by the snow reservoir only with the same fixed annual storage, thresholds, and flow constants. Using one reservoir with the same storage, threshold, flow constants in an Arctic glacial environment, however, seems useful despite its simplicity and indicates good accordance ($R^2 = 0.77$) between observed and modeled runoff, even though some discrepancies occur in runoff (Figures 4 and 6(a–d)). Simulated discharge tends to be overestimated during the main ablation period and underestimated at peak flows. For 1995, as the only year, simulated runoff is generally underestimated for the entire runoff period compared to other validation years (1993–1995 and 1998/1999) (Figure 6(c)), probably because of uncertainties in the 1995 yearly stage-discharge relationship.

Future NAM runoff simulations based on the IPCC A2 and B2 climate scenarios (2071–2100) indicate one and a half times higher yearly runoff (around 3200 mm w.eq. yr^{-1} with maximum monthly values around 900 mm w.eq.) than today (around 2000 mm w.eq. yr^{-1}). The increasing runoff is caused by the increasing negative glacier net mass balance from approximately -750 mm w.eq. yr^{-1} (1961–1990) to approximately -2000 mm w.eq. yr^{-1} (2071–2100), indicating an approximately three times higher negative glacier net mass balance than today. The increasing mean annual air temperature of approximately 1.4°C and related melting are more pronounced due to the high catchment glacier cover (14.4 km^2; 78%) than future changes in potential evapotranspiration and precipitation.

Conclusion

A lumped conceptual Rainfall–Runoff model, the NAM model, original developed for Danish catchments, which accounts for routing of water through different reservoirs, has been used to describe the variation in runoff from a glacierised and snow-covered catchment in SE Greenland. Despite the NAM model's simplicity this research had shown that the model seems to be useful ($R^2 = 0.77$) on the Mittivakkat Glacier catchment in quantifying intra- and inter-annual variation in runoff. Timing and magnitude of simulated discharge are in general in good accordance with observed discharge (1993–2004). Due to the lag of runoff values through winter daily photographic time lapse was effectively used for model calibration of simulated runoff through winter. In the future an increasing negative glacier net mass balance will occur from approximately -750 mm w.eq. yr^{-1} (1960–1990) to approximately -2000 mm w.eq. yr^{-1} (2071–2100) for both IPCC climate scenarios A2 and B2, indicating up to three times higher negative glacier net mass balance than today. Simulated runoff increases up to approximately 3200 mm w.eq. yr^{-1}, approximately one and a half times higher than today, highly based on increasing air temperature.

Acknowledgements

Special thanks go to Senior Scientist Ole Bøssing Christensen, Climate Research Division, Danish Meteorological Institute (DMI), for providing the HIRHAM RCM data. The authors would like to thank Professor Lars Bengtsson, Department of Water Resources Engineering, Lund University, and two anonymous reviewers for their insightful reviews of this paper. Thanks are also extended to Research Professor Jens Christian Refsgaard, Geological Survey of Denmark and Greenland (GEUS) and Associate Professor Carl Egede Bøggild, University Centre Svalbard (UNIS) for fruitful discussions. The project is supported partly by grants from the Danish Natural Science Research Council (SNF) (grant no. 21-03-0530) and partly from the Copenhagen Global Change Initiative (COGCI), University of Copenhagen.

References

ACIA (2005). *Arctic Climate Impact Assessment*, Cambridge University Press, Cambridge.

Anderson, E.A. (1976). A point energy balance model of a snow cover. *NOAA Tech. Rep. NWS*, 19.

Arnold, N.S., Willis, I.C., Sharp, M.J., Richards, K.S. and Lawson, W.J. (1996). A distributed surface energy-balance model for a small valley glacier. I. Development and testing for Haut Glacier d'Arolla, Valais, Switzerland. *J. Glaciol.*, **42**(140), 77–89.

Aslyng, H.C. and Hansen, S. (1982). *Water Balance and Crop Production, Model WATCROP for Local and Regional Application*, Hydrotechnical Laboratory, The Royal Veterinary and Agricultural University, Copenhagen.

Baker, D., Escher-Vetter, H., Moser, H., Oerter, H. and Reinwarth, O. (1982). A glacier discharge model based on results from field studies of energy balance, water storage and flow. *Hydrological Aspects of Alpine and High Mountain Areas (Procedings of the Exeter Symposium, July 1982). IAHS*, **138**, 103–112.

Bengtsson, L. and Singh, V.P. (2000). Model sophistication in relation to scales in snowmelt runoff modeling. *Nordic Hydrol.*, **31**(4/5), 267–286.

Bøggild, C.E. *En metode til beregning af genfrysning – langs en række profilerpå Amitsulooq Iskappen*. BSc Thesis University of Copenhagen, unpublished.

Bøggild, C.E. (2000). Preferential flow and melt water retention in cold snow packs in West-Greenland. *Nordic Hydrol.*, **31**(4/5), 287–300.

Bøggild, C.E., Forsberg, R. and Reeh, N. (2005). Melt water in a transect across the Greenland ice sheet. *Annal. Glaciol.*, **40**, 169–173.

Bøggild, C.E., Knudby, C.J., Knudsen, M.B., Pedersen, M.H., Starzer, W. and Thomsen, H.H. (1998). Modelsimulering af afstrømningen fra et arktisk bassin - Et pilotstudie til vurdering af arktiske vandressourcer. Danmarks og Grønlands Grologiske undersøgelser (in Danish). *Miljø- og Energiministeriet*, **43**, 67.

Bøggild, C.E., Knudby, C.J., Knudsen, M.B. and Starzer, W. (1999). Snowmelt and runoff modelling of an Arctic hydrological basin in west Greenland. *Hydrol, Process.*, **13**, 1989–2002.

Box, J.E. (2002). Survey of Greenland instrumental temperature records: 1973–2001. *Int. Climatol.*, **22**, 1829–1847.

Braithwaite, R.J. (1995). Positive degree-day factors for ablation on the Greenland ice sheet studies by energy-balance modelling. *J. Glaciol.*, **41**(137), 153–160.

Broecker, W.S. and Denton, G.H. (1990). The role of ocean-atmosphere reorganization in glacial cycles. *Quart. Sci. Rev.*, **9**, 305–341.

Broecker, W.S., Peteet, D.M. and Rind, D. (1985). Does the ocean-atmosphere system have more than one stable mode of operation. *Nature*, **315**, 21–26.

Brown, R.D., Brasnett, B. and Robinson, D. (2003). Gridded North American monthly snow depth and snow water equivalent for GCM evaluation. *Atmosphere-Ocean*, **41**(1), 1–14.

Bruland, O. and Killingtveit, Å. (2002). An energy balance based HBV-model with application to an Arctic watershed on Svalbard, Spitsbergen. *Nordic Hydrol.*, **33**(2), 123–144.

Bruland, O. and Sand, K. (1994). The Nordic HBV-model applied to an Arctic watershed. In *Proceedings of the 10th international Northern Research Basins Symposium and Workshop, Spitsbergen, Norway*, Sand, K. and Killingtveit, Å. (eds), SINTEF Rep. STF22 A96415. Norwegian Institute of Technology, Trondheim, pp. 594–608.

Campbell, W.I. and Rasmussen, L.A. (1973). The production, flow and distribution of meltwater in a glacier treated as a porous medium. *Hydrology of Glaciers (Proc. Cambridge Symp. Sept 1969). IAHS*, **95**, 11–27.

Christensen, J.H., Christensen, O.B., Lopez, P., Meijgaard, E.V. and Botzet, M. (1996). The HIRHAM4 Regional Atmospheric Climate Model. *DMI Scientific Report*, 1–19.

Christensen, J.H., Christensen, O.B., Schultz, J.-P., Hagemann, S. and Botzet, M. (2001). *High Resolution Physiographic Data Set for HIRHAM4: An Application to a 50 km Horizontal Resolution Domain Covering Europe*, 01–15DMI Technical Report.

Colbeck, S.C. (1974). The capillary effects on water percolation in homogeneous snow. *Journal of Glaciology*, **13**(67), 85–97.

Conway, H. and Benedict, R. (1994). Infiltration of water into snow. *Wat. Res. Res.*, **30**(3), 641–649.

Crowely, T.J. (2000). Causes of climate change over the the past 1000 years. *Sci. Tech. Froid*, **289**(5477), 270–277.

de Bruin, H.A.R. and Lablans, W.N. (1998). Reference crop evapotranspiration determined with a modified Makkink equation. *Hydrol. Process.*, **12**(7), 1053–1062.

DHI Water and Environment (2003a). *MIKE 11 Reference Manual*, DHI Water and Environment, Denmark.

DHI Water and Environment (2003b). *MIKE 11 User Guide*, DHI Water and Environment, Denmark.

Dowdeswell, J.A., Hagen, J.O., Björnsson, H., Glazovsky, A.F., Harrison, W.D., Holmlund, P., Jania, J., Koerner, R.M., Lefauconnier, B., Ommanney, C.S.L. and Thomas, R.H. (1997). The mass balance of circum-Arctic glaciers and recent climate change. *Quat. Res.*, **48**(1–4), 1–14, no. QR971900.

Dubrovský, M., Žalud, Z., Trnka, M., Pešice, P. and Haberle, J. (2002). Perun - the system for the crop yield forecasting. In: *XIV Česko-Slovenská Bioklimatologická Konference, Lednice, Czech Republic, 2–4 September, 2002*. pp. 1–10.

Flato, G.M. and Boer, G.J. (2001). Warming asymmetry in climate change simulations. *Geophys. Res. Lett.*, **28**, 195–198.

Fountain, A.G. and Walder, J.S. (1998). Water transit through temperate glaciers. *Rev. Geophys.*, **36**(3), 299–328.

Fountain, A.G., Jacobel, R.W., Schlichting, R. and Jansson, P. (2005). Fractures: a new paradigm for englacial water flow. *Nature*, **433**, 618–621.

Fristrup, B. (1961). Studies of four glasciers in Greenland. *Danish Journal of Geography*, **59**, 89–102.

Garen, D.C. and Marks, D. (2005). Spatially distributed energy balance snowmelt modelling in a mountainous river basin: estimation of meteorological inputs and verification of model results. *J. Hydrol.*, **315**, 126–153.

Gordon, C., Cooper, C., Senior, C.A., Banks, H., Gregory, J.M., Johns, T.C., Mitchell, J.F.B. and Wood, R.A. (2000). The simulation of SST, sea ice extents and ocean heat transports in a version of the Hadley Centre coupled model without flux adjustments. *Climate Dyn.*, **16**, 147–168.

Gottlieb, L. (1980). Development and applications of a runoff model for snowcovered and glacierized basins. *Nordic Hydrol.*, **11**, 255–272.

Hag, M.P., Bille-Hansen, J. and Olesen, O.B. (2001). Arktiske vandressourcer - fysisk baseret modelværktøj. *Greenland Survey, ASIAQ (in Danish)*, **2001–2**, 1–49.

Hasholt, B. (1980). Morphological and hydrological possibilities for the development of water power at Angmagssalik – a case study of applied physical geography. *Geograf. Tidsskrift/Dan. J. Geogr.*, **80**, 57–62.

Hasholt, B. (1986). Kortlægning af Midtluagkat Gletscheren og nogle hydro-glaciologiske observationer (in Danish). *Geograf. Tidsskrift/Dan. J. Geogr.*, **86**, 9–16.

Hasholt, B. (1988). Massbalance studies of the Midtluagkat Glacier, Eastern Greenland. Geograf. *Tidsskrift/Dan. J. Geogr.*, **88**, 82–85.

Hasholt, B. (1992). Sediment transport in a proglacial valley, Sermilik, East Greenland. *Geograf. Tidsskrift/Dan. J. Geogr.*, **86**, 105–110.

Hasholt, B., Liston, G.E. and Knudsen, N.T. (2003). Snow-distribution modelling in the Ammassalik Region, South East Greenland. *Nordic Hydrol.*, **34**(1/2), 1–16.

Hasholt, B. and Mernild, S.H. (2004). Estimation of water balance in and around the Mittivakkat Glacier basin, Ammassalik Island, Southeast Greenland. *Northern Research Basins Water Balance. IAHS*, **290**, 129–142.

Hock, R. (1999). A distributed temperature-index ice- and snowmelt model including potential direct solar radiation. *J. Glaciol.*, **45**(149), 101–111.

Hock, R. (2003). Temperature index melt modelling in mountain areas. *J. Hydrol.*, **282**, 104–115.

Hock, R. and Hoetzli, C. (1997). Areal melt and discharge modelling of Storglaciären, Sweden. *International Symposium on Changing Glaciers, Fjærland, Norway, 24–27 June. Annal. Glaciol.*, **24**, 211–216.

Hoch, R. and Hooke, R.L. (1993). Evolution of the internal drainage system in the lower part of the ablation area of Storglaciären, Sweden. *Geol. Soc. Am. Bull.*, **105**, 537–546.

Hock, R. and Jansson, P. (2005). Modelling glacier hydrology. In *Encyclopedia of Hydrological Science*, Andersen, M. (ed.), John Wiley and Sons, New York, pp. 1–9.

Hirashima, H., Ohata, T., Kodama, Y. and Yabuki, H. (2004). Estimation of annual water balance in Siberian tundra using a new land surface model. *Northern Research Basins Water Balance. IAHS*, **290**, 41–49.

Jacobs, A.F.G. and de Bruin, H.A.R. (1998). Makkink's equation for evapotranspiration applied to unstressed maize. *Hydrol. Process*, **12**(7), 1063–1066.

Jansson, P., Hock, R. and Schneider, T. (2003). The concept of glacier storage: a review. *J. Hydrol.*, **282**, 116–129.

Kane, D.L. (1997). The impact of hydrologic perturbation on arctic ecosystems induced by climate change. global change and Arctic terrestrial ecosystems. *Ecol. Stud.*, **124**, 63–81.

Kane, D.L. and Yang, D. (2004). Overview of water balance determinations for high latitude watersheds. *Northern Research Basins Water Balance. IAHS*, **290**, 1–12.

Klemes, V. (1985). *Sensitivity of Water Resources Systems to Climate Variations*, World Meteorological Organisation, Geneva, WPC Rep. No. 98.

Klemes, V. (1986). Operationel testing of hydrological simulation models. *Hydrol. Sci. J.*, **31**(1), 13–24.

Knudsen, N.T. and Hasholt, B. (1999). Radio-echo sounding at the Mittivakkat Gletscher, Southeast Greenland. *Arctic Antarctic Alp. Res.*, **31**(3), 321–328.

Knudsen, N.T. and Hasholt, B. (2004). Mass balance observations at the Mittivakkat Gletscher, Southeast Greenland 1995-2002. *Nordic Hydrol.*, **35**(4–5), 381–390.

Kuhn, M. (2003). Redistribution of snow and glacier mass balance from a hydrometeorological model. *J. Hydrol.*, **282**, 95–103.

Liston, G.E. and Elder, K. (2005). A distributed snow-evolution modeling system (SnowModel). *J. Hydrometeorol*., in press.

Makkink, G.F. (1957). Ekzameno de la formula de Penman. *Neth. J. Agric. Sci.*, **5**, 290–305.

Marsh, P. (1999). Snowcover formation and melt: recent advances and future prospects. *Hydrol. Process.*, **13**, 2117–2134.

Marsh, P. and Woo, M.-K. (1984). Wetting front advance and freezing of meltwater within a snow cover – a simulating model. *Wat. Res. Res.*, **20**(12), 1865–1874.

Maxwell, B. (1997). Recent climate patterns in the Arctic. Global change and Arctic terrestrial ecosystems. *Ecol. Stud.*, **124**, 21–47.

Mernild, S.H. (2006). The internal drainage system of lower Mittivakkat Glacier, Ammassalik Island, Southeast Greenland. *Dan. J. Geogr.*, **106**(1), 13–24.

Mernild, S.H., Hasholt, B. and Hansen, B.U. (2005). Meteorological observations 2003 at the Sermilik Station, Ammassalik Island, Southeast Greenland. *Dan. J. Geogr.*, **105**(2), 49–56.

Mernild, S.H., Hasholt, B. and Liston, G.E. (2006a). Water flow through Mittivakkat Glacier, Ammassalik Island, SE Greenland. *Dan. J. Geogr.*, **106**(1), 25–42.

Mernild, S.H., Liston, G.E., Hasholt, B. and Knudsen, N.T. (2006b). Snow-distribution and melt-modeling at the Mittivakkat Glacier, Sermilik, Eastern Greenland. *J. Hydrometeorol.*, **7**, 808–824.

Nielsen, S.A. and Hansen, E. (1973). Numerical simulation of the rainfall runoff process on a daily basis. *Nordic Hydrol.*, **4**, 171–190.

Plauborg, F., Refsgaard, J.K., Henriksen, H.J., Blicher-Mathiasen, G. and Kern-Hansen, C. (2002). *Vandbalance på mark- og oplandsskala (in Danish)*. Foulum Rapport 5-02-02.

Pope, V.D., Gallani, M.L., Rowntree, P.R. and Stratton, R.A. (2000). The impact of new physical parametrizations in the Hadley Centre climate model - HadAM3. *Climate Dyn.*, **16**, 123–146.

Refsgaard, J.C. (2000). Towards a formal approach to calibration and validation of models using spatial data. In *Spatial Patterns in Catchment Hydrology: Observations and Modelling*, Gryson, R. and Blöschl, G. (eds), Cambridge University Press, Cambridge, pp. 329–354.

Refsgaard, J.C. and Henriksen, H.J. (2004). Modelling guidelines – terminology and guiding principles. *Adv. Wat. Res.*, **27**, 71–82.

Refsgaard, J.C. and Knudsen, J. (1996). Operational validation and intercomparison of different types of hydrological models. *Wat. Res. Res.*, **32**(7), 2189–2202.

Röthlisberger, H. (1972). Water pressure in intra- and subglacial channels. *J. Glaciol.*, **11**(62), 177–203.

Röthlisberger, H. and Lang, H. (1987). Glacier hydrology. In *Glaciofluvial Sediment Transfer*, Grunell, A.M. and Clark, M.J. (eds), Wiley, New York, pp. 207–284.

Rysgaard, S., Vang, T., Stjernholm, M., Rasmussen, B., Windelin, A. and Kiilsholm, S. (2003). Physical conditions, carbon transport, and climate change impacts in a Northeast Greenland Fjord. *Arctic Antarctic Alp. Res.*, **35**, 301–312.

Sælthun, N.R. and Barkved, L.J (2003). Climate Changes Secnarios for the SCANNET Region. Norwegian Institute for Water Research, Report no. 4663, pp. 1–70.

Serreze, M.C., Maslanik, J., Scambos, T.A., Fetterer, F., Stroeve, J., Knowles, K., Fowler, C., Drobot, S., Barry, R. and Haran, T.M. (2002). A record minimum arctic sea ice extent and area in 2002. *Geophys. Res. Lett*, **30**(3), 1110, doi:10.1029/2002GL016406.

Shreve, R.L. (1972). Movement of water in glaciers. *J. Glaciol.*, **11**(62), 205–214.

Sturm, M., Schimel, J., Michaelson, G., Welker, J.M., Oberbauer, S.F., Liston, G.E., Fahnestock, J. and Romanovsky, V.E. (2005). Winter biological processes could help convert Arctic tundra to shrubland. *Bio Science*, **55**(1), 17–26.

Tangborn, W.V. (1984). Prediction of glacier derived runoff for hydroelectric development. *Geogr. Annal.*, **66A**(3), 257–265.

Trabant, D.C. and Mayo, L.R. (1985). Estimation and effects of internal accumulation on five glaciers in Alaska. *Annal. Glaciol.*, **6**, 113–117.

Valeur, H. (1959). Run-off studies from the Mitdluagkat Gletscher in SE-Greenland during the late summer 1958. *Geograf. Tidsskrift (Dan. J. Geogr.*, **58**, 54–65.

Van de Wal, R.S.W. and Russell, A.J. (1994). A comparison of energy balance calculations, measured ablation and meltwater runoff near Sønder Strømfjord, West Greenland. *Global Planet. Change*, **9**, 29–38, Available at: http://www.ipcc.ch: Intergovernmental Panel on Climate Change.

WHO (2001). WHO statement on the status of the global climate in 2001. *WHO#670*. World Meteorological Organization, Geneva, Switzerland.